

Reduced basis isogeometric mortar approximations for eigenvalue problems in vibroacoustics ^{*}

THOMAS HORGER[†], BARBARA WOHLMUTH[‡], LINUS WUNDERLICH[§]
 Institute for Numerical Mathematics, Technische Universität München,
 Boltzmannstraße 3, 85748 Garching b. München, Germany

Abstract

We simulate the vibration of a violin bridge in a multi-query context using reduced basis techniques. The mathematical model is based on an eigenvalue problem for the orthotropic linear elasticity equation. In addition to the nine material parameters, a geometrical thickness parameter is considered. This parameter enters as a 10th material parameter into the system by a mapping onto a parameter independent reference domain. The detailed simulation is carried out by isogeometric mortar methods. Weakly coupled patch-wise tensorial structured isogeometric elements are of special interest for complex geometries with piecewise smooth but curvilinear boundaries. To obtain locality in the detailed system, we use the saddle point approach and do not apply static condensation techniques. However within the reduced basis context, it is natural to eliminate the Lagrange multiplier and formulate a reduced eigenvalue problem for a symmetric positive definite matrix. The selection of the snapshots is controlled by a multi-query greedy strategy taking into account an error indicator allowing for multiple eigenvalues.

1 Introduction

Eigenvalue problems in the context of vibroacoustics often depend on several parameters. In this work, we consider a geometry and material dependent violin bridge. For a fast and reliable evaluation in the real-time and multi-query context, reduced basis methods have proven to be a powerful tool.

For a comprehensive review on reduced basis methods, see, e. g., [30, 34] or [29, Chapter 19] and the references therein. The methodology has been applied successfully to many different problem classes, among others Stokes problems [21, 22, 33, 35], variational inequalities [14, 16] and linear elasticity [24]. Recently, reduced basis methods for parameterized elliptic eigenvalue problems (μ EVs) gained attention.

^{*}We would like to gratefully acknowledge the funds provided by the Deutsche Forschungsgemeinschaft under the contract/grant numbers: WO 671/11-1, WO 671/13-2 and WO 671/15-1 (within the Priority Programme SPP 1748, "Reliable Simulation Techniques in Solid Mechanics. Development of Non-standard Discretisation Methods, Mechanical and Mathematical Analysis").

[†]Corresponding author. E-Mail: horger@ma.tum.de

[‡]wohlmuth@ma.tum.de

[§]linus.wunderlich@ma.tum.de

Early work on a residual a posteriori estimator for the first eigenvalue can be found in [23] and has been generalized in [26, 27, 28] to the case of several single eigenvalues with special focus to applications in electronic structure problems in solids. Furthermore, the very simple and special case of a single eigenvalue where only the mass matrix and not the stiffness matrix of a generalized eigenvalue problem is parameter dependent has been discussed in [12]. Alternatively to the classical reduced basis approach, component based reduction strategies are considered in [37]. Here, we follow the ideas of [18] where rigorous bounds in the case of multi-query and multiple eigenvalues are given.

More precisely, a single reduced basis is built for all eigenvalues of interest, based on a greedy selection using an online-offline decomposable error estimator.

The eigenvalues of a violin bridge play a crucial role in transmitting the vibration of the strings to the violin body and hence influence the sound of the instrument, see [11, 38]. Due to the complicated curved domain and improved eigenvalue approximations compared to finite element methods, see [20], we consider an isogeometric discretization. Flexibility for the tensor product spline spaces are gained by a weak domain decomposition of the non-convex domain.

Isogeometric analysis, introduced in 2005 by Hughes et al. in [19], is a family of methods that uses B-splines and non-uniform rational B-splines (NURBS) as basis functions to construct numerical approximations of partial differential equations, see also [1, 6]. Mortar methods are a popular tool for the weak coupling of non-matching meshes, originally introduced for spectral and finite element methods [2, 3, 4]. An early contribution to isogeometric elements in combination with domain decomposition techniques can be found in [17]. A rigorous mathematical analysis of the a priori error in combination with uniform stability results for different Lagrange multiplier spaces is given in [5] and applications of isogeometric mortar methods can be found in [8, 9, 36].

Mortar formulations are quite often formulated as an indefinite saddle point-problem. The additional degrees of freedom for the Lagrange multiplier as well as the need for a uniform inf-sup condition to achieve stability make mortar methods, in general, more challenging than simple conforming approaches. Theoretically, the Lagrange multiplier can be eliminated. However this often results in a global process and is not carried out directly. While this concerns the detailed solution, the reduced basis can be purely based on a primal space and results in a non-conforming but positive definite approach. Then the saddle point structure becomes redundant, and we gain the efficiency of a positive definite reduced system.

This article is structured as follows. In Section 2, we describe the geometric setup and the isogeometric mortar discretization for the violin bridge. The model order reduction is introduced in Section 3, including a modified error estimator. Numerical results illustrating the accuracy and flexibility of the presented approach are given in Section 4.

2 Problem setting

In vibroacoustical applications, often complicated curved domains are of special interest. Besides large constructions, such as bridges and buildings, also music instruments are investigated. An important part of the violin is a wooden violin bridge, depicted in

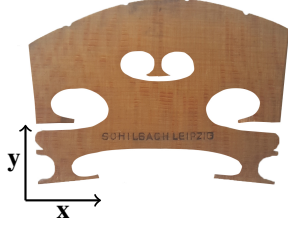


Figure 1: Example of a violin bridge.

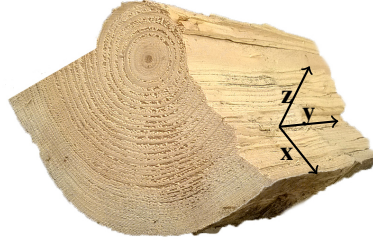


Figure 2: Illustration of the orthotropic structure of wood.

Figure 1. For this geometry, we consider the eigenvalue problem of elasticity

$$-\operatorname{div} \sigma(u) = \lambda \rho u,$$

where $\rho > 0$ is the mass density, and $\sigma(u)$ depends on the material law of the structure under consideration. In our case, linear orthotropic materials are appropriate since as depicted in Figure 2 wood consists of three different axes and only small deformations are considered. Note that besides the cylindrical structure of a tree trunk, we consider Cartesian coordinates due to the comparably small size of the bridge.

2.1 Orthotropic material law

The three axes are given by the fiber direction y , the in plane orthogonal direction z and the radial direction x . By Hooke's law, the stress strain relation can be stated in its usual form as $\sigma(u) = \mathbb{C}\varepsilon(u)$ with $\varepsilon(u) = (\nabla u + \nabla u^\top)/2$. Due to the alignment of the coordinate system with the orthotropic structure, the stiffness tensor is given as

$$\mathbb{C} = \begin{pmatrix} A_{11} & A_{12} & A_{13} & 0 & 0 & 0 \\ A_{21} & A_{22} & A_{23} & 0 & 0 & 0 \\ A_{31} & A_{32} & A_{33} & 0 & 0 & 0 \\ 0 & 0 & 0 & G_{yz} & 0 & 0 \\ 0 & 0 & 0 & 0 & G_{zx} & 0 \\ 0 & 0 & 0 & 0 & 0 & G_{xy} \end{pmatrix}, \quad (1)$$

with the shear moduli G_{xy}, G_{yz}, G_{zx} and the entries A_{ij} depending on the elastic moduli E_x, E_y, E_z and the Poisson's ratios $\nu_{xy}, \nu_{yz}, \nu_{zx}$. The exact formula for A_{ij} can be found in [31, Chapter 2.4].

Some important differences compared to isotropic material laws are worth pointing out. While in the isotropic case, all Poisson's ratios share the same value, for orthotropic materials they represent three independent material parameters. The only relation between the ratios is $\nu_{ij}E_j = \nu_{ji}E_i$. Also the possible range of the material parameters, i.e., $-1 < \nu < 1/2$ for the isotropic case, is different. $1 > \nu_{yz}^2 E_z/E_y + \nu_{xy}^2 E_y/E_x + 2\nu_{xy}\nu_{yz}\nu_{zx}E_z/E_x + \nu_{zx}^2 E_z/E_x$ and $E_x/E_y > \nu_{xy}^2$ are necessary for a positive definite stiffness tensor and hence a coercive energy functional. Note that Poisson's ratios larger than $1/2$ are permitted, but this does not imply unphysical behavior as in the isotropic case, see, e.g., [32]. The conditions $E_i, G_{ij} > 0$ hold both in the isotropic and orthotropic case.

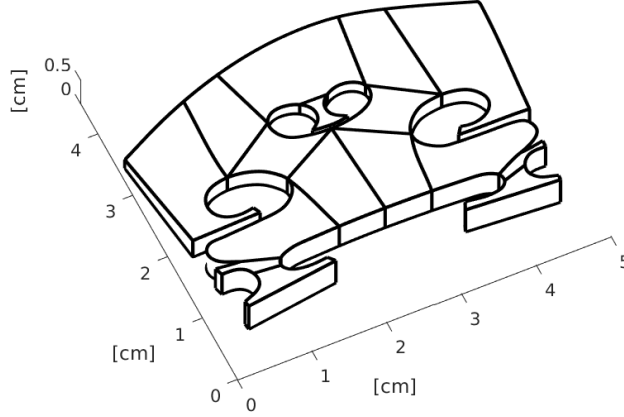


Figure 3: Decomposition of the three-dimensional geometry into 16 patches and 16 interfaces.

The curved domain of the violin bridge can be very precisely described by a spline volume. Since it is not suitable for a single-patch description, we decompose it into 16 three-dimensional spline patches shown in Figure 3. While the description of the geometry could also be done with fewer patches, the number of 16 patches Ω_i gives us regular geometry mappings and a reasonable flexibility of the individual meshes. The decomposed geometry is solved using an equal-order isogeometric mortar method as described in [5]. A trivariate B-spline space V_i is considered on each patch Ω_i . The broken ansatz space $V_h = \prod_i V_i$ is weakly coupled on each of the 16 interfaces. For each interface γ_k the two adjacent domains are labeled as one slave and one master domain (i.e. $\gamma_k = \partial\Omega_s \cap \partial\Omega_m$) and the coupling space M_k is set as the trace space of the spline spaces on the slave domain and $M_h = \prod_k M_k$. Several crosspoints are present in the decomposition, where an appropriate local degree reduction is performed, as described in [5, Section 4.3], to guarantee stability.

We use the standard bilinear forms for mortar techniques in linear elasticity

$$a(u, v) = \sum_i \int_{\Omega_i} \sigma(u) : \varepsilon(v), \quad m(u, v) = \sum_i \int_{\Omega_i} \rho uv, \quad b(v, \hat{\tau}) = \sum_k \int_{\gamma_k} [v]_k \hat{\tau},$$

where $[v]_k = v_s|_{\gamma_k} - v_m|_{\gamma_k}$ denotes the jump across the interface γ_k . We note that no additional variational crime by different non-matching geometrical resolutions of γ_k enters. The detailed eigenvalue problem is defined as $(u, \tau) \in V_h \times M_h$, $\lambda \in \mathbb{R}$, such that

$$a(u, v) + b(v, \tau) = \lambda m(u, v), \quad v \in V_h, \quad (2a)$$

$$b(u, \hat{\tau}) = 0, \quad \hat{\tau} \in M_h. \quad (2b)$$

The Lagrange multiplier τ is an approximation for the surface tension $\sigma(u)n$ along the interfaces.

Additional to the nine material parameters E_i, G_{ij}, ν_{ij} , we consider a geometry parameter μ_{10} , describing the thickness of the violin bridge. Transforming the geometry to a reference domain, we can interpret the thickness parameter as one more material parameter.

2.2 Transforming geometrical parameters to material parameters

Let the parameter dependent geometry $\Omega(\mu)$ be an unidirectional scaling of a reference domain $\widehat{\Omega}$, i.e., a transformation by $F(\cdot; \mu) : \widehat{\Omega} \rightarrow \Omega(\mu)$, $\mathbf{x} = F(\widehat{\mathbf{x}}; \mu) = (\widehat{x}, \widehat{y}, \mu_{10}\widehat{z})$, with $\widehat{\mathbf{x}} = (\widehat{x}, \widehat{y}, \widehat{z}) \in \widehat{\Omega}$. Transforming the unknown displacement and rescaling it as $\widehat{u}(\widehat{\mathbf{x}}) = DF(\widehat{\mathbf{x}}; \mu)u(F(\widehat{\mathbf{x}}; \mu))$ allows us to define a symmetric strain variable on the reference domain

$$\widehat{\boldsymbol{\varepsilon}}(\widehat{u}(\widehat{\mathbf{x}})) = DF(\widehat{\mathbf{x}}; \mu)\boldsymbol{\varepsilon}(u(F(\widehat{\mathbf{x}}; \mu)))DF(\widehat{\mathbf{x}}; \mu).$$

The orthotropic stiffness tensor (1) is then transformed to

$$\widehat{\mathbb{C}}(\mu) = \begin{pmatrix} A_{11} & A_{12} & \mu_{10}^{-2}A_{13} & & & \\ A_{21} & A_{22} & \mu_{10}^{-2}A_{23} & & & \\ \mu_{10}^{-2}A_{31} & \mu_{10}^{-2}A_{32} & \mu_{10}^{-4}A_{33} & & & \\ & & & \mu_{10}^{-2}G_{yz} & & \\ & & & & \mu_{10}^{-2}G_{zx} & \\ & & & & & G_{xy} \end{pmatrix}.$$

In terms of this coordinate transformation, the eigenvalue problem in the continuous H^1 -setting reads, since $\det DF(\widehat{\mathbf{x}}; \mu) = \mu_{10}^{-1}$ is constant, as

$$\int_{\widehat{\Omega}} \widehat{\boldsymbol{\varepsilon}}(\widehat{u}) \widehat{\mathbb{C}}(\mu) \widehat{\boldsymbol{\varepsilon}}(\widehat{v}) \, d\widehat{\mathbf{x}} = \lambda \int_{\Omega} \rho \widehat{u}^\top \begin{pmatrix} 1 & & \\ & 1 & \\ & & \mu_{10}^{-2} \end{pmatrix} \widehat{v} \, d\widehat{\mathbf{x}}.$$

In our mortar case, the coupling conditions across the interfaces have to be transformed as well. However due to the affine mapping with respect to x , y and z , the parameter dependency on $b(\cdot, \cdot)$ can be removed.

Another material parameter of interest for applications is the constant mass density ρ . However any change in the constant ρ does not influence the eigenvectors. Only the eigenvalue is rescaled, yielding a trivial parameter dependence. For this reason, the density is kept constant in the reduced basis computations and can be varied in a postprocess by rescaling the eigenvalues.

The described material parameters allow for an affine parameter dependence of the mass and the stiffness, with $Q_a = 10$, $Q_m = 2$,

$$a(\cdot, \cdot; \mu) = \sum_{q=1}^{Q_a} \theta_a^q(\mu) a^q(\cdot, \cdot), \quad m(\cdot, \cdot; \mu) = \sum_{q=1}^{Q_m} \theta_m^q(\mu) m^q(\cdot, \cdot).$$

3 Reduced Basis

Reduced basis methods for the simultaneous approximation of eigenvalues and eigenvectors have been analyzed in [18]. Here, we apply these methods to the previously described setting. An important difference to the previous work is that we wish to approximate a saddle point problem instead of a positive definite matrix.

Previous works on saddle point problems construct a reduced basis for both the primal and the dual space. This is necessary for example for variational inequalities or when the coupling is parameter dependent, see [13, 15, 16, 25]. To ensure the inf-sup stability of the discrete saddle point problem, supremizers can be added to the primal space, additionally increasing the size of the reduced system.

3.1 Reduction of the saddle point problem

Due to the parameter-independence of $b(\cdot, \cdot)$, we can reformulate the detailed saddle point problem (2) in a purely primal form posed on the constrained space $X_h = \{v \in V_h, b(v, \widehat{\tau}) = 0, \widehat{\tau} \in M_h\}$. Note that this formulation is not suitable for solving the detailed solution, since, in general, it is costly to construct a basis of X_h and severely disturbs the sparsity of the detailed matrices. Only in the case of so-called dual Lagrange multiplier spaces, a local static condensation can be carried out and the constrained basis function do have local support. However, in the reduced basis context the constructed basis functions do automatically satisfy the weak coupling properties and thus the saddle-point problem is automatically reduced to a positive definite one.

Our reduced space is defined by $X_N = \{\zeta_n \in X_h, n = 1, \dots, N\}$, where the reduced basis functions ζ_n are selected as presented in [18]. Then the reduced eigenvalue problem for the first K eigenpairs is given by: Find the eigenvalues $\lambda_{\text{red},i}(\mu) \in \mathbb{R}$ and the eigenfunctions $u_{\text{red},i}(\mu) \in X_N, i = 1, \dots, K$, such that

$$a(u_{\text{red},i}(\mu), v; \mu) = \lambda_{\text{red},i}(\mu) m(u_{\text{red},i}(\mu), v; \mu), \quad v \in X_N$$

In a first step, an initial basis is built by a small POD. This basis is then enlarged by a greedy algorithm with an asymptotically reliable error estimator.

3.2 Decomposition of the error estimator with a parameter-dependent mass

The error estimator presented in [18, Corollary 3.3] can directly be applied, but the online-offline decomposition needs to be modified. In the original setting, a parameter-independent mass was considered, so we need to additionally include the affine decomposition of the mass matrix.

The main contribution of the estimator is the residual

$$r_i(\cdot; \mu) = a(u_{\text{red},i}(\mu), \cdot; \mu) - \lambda_{\text{red},i}(\mu) m(u_{\text{red},i}(\mu), \cdot; \mu)$$

measured in the dual norm $\|r\|_{\widehat{\mu}; X_h'} = \sup_{v \in X_h} r(v) / \widehat{a}(v, v)^{1/2}$, where $\widehat{a}(u, v) := a(u, v; \widehat{\mu})$, and $\widehat{\mu} \in \mathcal{P}$ is a reference parameter. We define $\widehat{e}_i(\mu) \in X_h$ by

$$a(\widehat{e}_i(\mu), v; \mu) = r_i(v; \mu), \quad v \in X_h.$$

To adapt the online-offline decomposition, we follow [18, 23] and add additional terms corresponding to the mass components m_q . Let $(\zeta_n)_{1 \leq n \leq N}$ be the orthonormal basis (w. r. t. $m(\cdot, \cdot; \widehat{\mu})$) of X_N and let us define $\xi_n^q \in X_N$ and $\xi_n^{m,q} \in X_N$ by

$$\begin{aligned} \widehat{a}(\xi_n^q, v) &= a^q(\zeta_n, v), \quad v \in X_h, \quad 1 \leq n \leq N, \quad 1 \leq q \leq Q_a, \\ \widehat{a}(\xi_n^{m,q}, v) &= m^q(\zeta_n, v), \quad v \in X_h, \quad 1 \leq n \leq N, \quad 1 \leq q \leq Q_m. \end{aligned}$$

In the following, we identify the function $u_{\text{red},i}(\mu) \in V_N$ and its vector representation w. r. t. the basis $(\zeta_n)_{1 \leq n \leq N}$ such that $(u_{\text{red},i}(\mu))_n$ denotes the n -th coefficient. Then, given a reduced eigenpair $(u_{\text{red},i}(\mu), \lambda_{\text{red},i}(\mu))$, we have the error representation

$$\widehat{e}_i(\mu) = \sum_{n=1}^N \sum_{q=1}^{Q_a} \theta_a^q(\mu) (u_{\text{red},i}(\mu))_n \xi_n^q - \lambda_{\text{red},i}(\mu) \sum_{n=1}^N \sum_{q=1}^{Q_m} \theta_m^q(\mu) (u_{\text{red},i}(\mu))_n \xi_n^{m,q}.$$

Consequently, the main contribution of $\eta_i(\mu)$ decomposes using $\|r_i(\cdot; \mu)\|_{\widehat{\mu}; X_h'}^2 = \widehat{a}(\widehat{e}_i(\mu), \widehat{e}_i(\mu))$, see [18, Section 3.3] for a more detailed discussion.

	E_x [MPa]	E_y [MPa]	E_z [MPa]	G_{yz} [MPa]	G_{zx} [MPa]	G_{xy} [MPa]	ν_{yz}	ν_{zx}	ν_{xy}
$\hat{\mu}$	14,000	2,280	1,160	465	1,080	1,640	0.36	0.0429	0.448
\mathcal{P}_1	13,000	1,500	750	100	500	1,000	0.3	0.03	0.4
	-15,000	-3,000	-1,500	-1,000	-1,500	-2,000	-0.4	-0.06	-0.5
\mathcal{P}_2	1,000	100	100	10	100	100	0.1	0.01	0.3
	-20,000	-5,000	-2,000	-5,000	-2,500	-5,000	-0.5	-0.1	-0.5

Table 1: Reference parameter and considered parameter ranges.

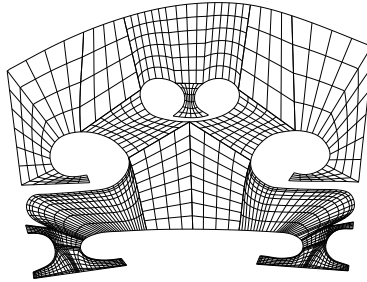


Figure 4: Non-matching isogeometric mesh of the violin bridge.

4 Numerical simulation

In this section, the performance of the proposed algorithm is illustrated by numerical examples. The detailed computations were performed using *geoPDEs* [7], a Matlab toolbox for isogeometric analysis, the reduced computations are based on *RBmatlab* [10].

For the detailed problem, we use an anisotropic discretization. In plane, we use splines of degree $p = 3$ on the non-matching mesh shown in Figure 4. The mesh has been adapted locally to better resolve possible corner singularities of the solution. In the z -direction a single element of degree $p = 4$ is used. The resulting equation system has 45,960 degrees of freedom for the displacement whereas the surface traction on the interfaces is approximated by 2,025 degrees of freedom.

We consider the ten parameters, described in Section 2, $\mu = (\mu_1, \dots, \mu_{10})$ with the elastic moduli $\mu_1 = E_x$, $\mu_2 = E_y$, $\mu_3 = E_z$, the shear moduli $\mu_4 = G_{yz}$, $\mu_5 = G_{xz}$, $\mu_6 = G_{xy}$, Poisson's ratios $\mu_7 = \nu_{yz}$, $\mu_8 = \nu_{xz}$, $\mu_9 = \nu_{xy}$ and the scaling of the thickness μ_{10} .

The considered parameter values were chosen according to real parameter data given in [32, Table 7-1]. We consider two different scenarios. In the first setting, we fix the wood type and take into account only natural variations, see [32, Section 7.10]. To capture the sensitivity of the violin bridge, one can choose a rather small parameter range around a reference parameter. We chose the reference data of *fagus sylvatica*, the common beech, as given in Table 1, as well as the parameter range \mathcal{P}_1 . The mass density is fixed in all cases as 720 kg/m^3 .

In our second test setting, we also consider different wood types. Hence we also consider a larger parameter set, including the parameters for several types of wood. Based on a selection of some wood types, we chose the parameter range \mathcal{P}_2 , see

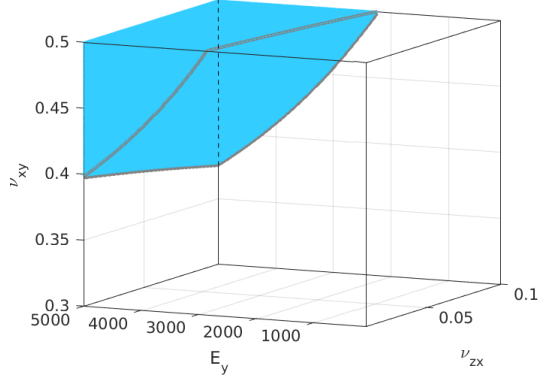


Figure 5: Illustration of non-admissible parameter values in a lower-dimensional excerpt of \mathcal{P}_2 , varying $\nu_{zx} \in (0.01, 0.1)$, $\nu_{xy} \in (0.3, 0.5)$, $E_y \in (100, 5000)$ and fixing $E_x = 1000$, $E_z = 2000$ and $\nu_{yz} = 0.5$.

Table 1. We note, that not all parameters in this large range are admissible for the orthotropic elasticity as they do not fulfill the conditions for the positive definiteness of the elastic tensor, stated in Section 2.1. Thus, we constrain the tensorial parameter space by

$$1 - \nu_{yz}^2 E_z / E_y + \nu_{xy}^2 E_y / E_x + 2\nu_{xy} \nu_{yz} \nu_{zx} E_z / E_x + \nu_{zx}^2 E_z / E_x \geq c_0,$$

as well as $E_x / E_y - \nu_{xy}^2 \geq c_1$ where the tolerances c_0 and c_1 were chosen according to several wood types. Exemplary, in Figure 5 we depict a lower-dimensional excerpt of \mathcal{P}_2 which includes non-admissible parameter values.

Eigenvalue	$\mu_{10} = 0.5$	$\mu_{10} = 1.0$	$\mu_{10} = 2.0$	ratio 0.5/1.0	ratio 1.0/2.0
1	0.4057	1.3238	3.6954	0.3065	0.3582
2	1.1613	3.8870	10.8071	0.2988	0.3597
3	4.4096	12.9562	26.5621	0.3403	0.4878
4	6.1371	19.3254	30.0050	0.3176	0.6441
5	13.5564	27.3642	53.2657	0.4954	0.5137
6	19.2229	46.2521	93.9939	0.4156	0.4921
7	27.6118	65.0940	111.6075	0.4242	0.5832
8	39.3674	96.8069	129.3406	0.4067	0.7485
9	57.8266	107.6749	189.6090	0.5370	0.5679
10	68.0131	130.8876	241.7695	0.5196	0.5414

Table 2: The 10 smallest eigenvalues for different thickness parameters, with the other parameters fixed to the reference value.

First, we consider the effect of the varying thickness parameter on the solution of our model problem. In Table 2 the first eigenvalues are listed for different values of the thickness, where we observe a notable and nonlinear parameter dependency. A selection of the corresponding eigenfunctions is depicted in Figure 6, where the strong influence becomes even more evident, since in some cases the shape of the eigenmode changes when varying the thickness.

In the following reduced basis tests, the relative error values are computed as the mean value over a large amount of random parameters. The L^2 -error of the normed eigenfunctions is evaluated as the residual of the L^2 -projection onto the corresponding detailed eigenspace. This takes into account possible multiple eigenvalues and the invariance with respect to a scaling by (-1) .

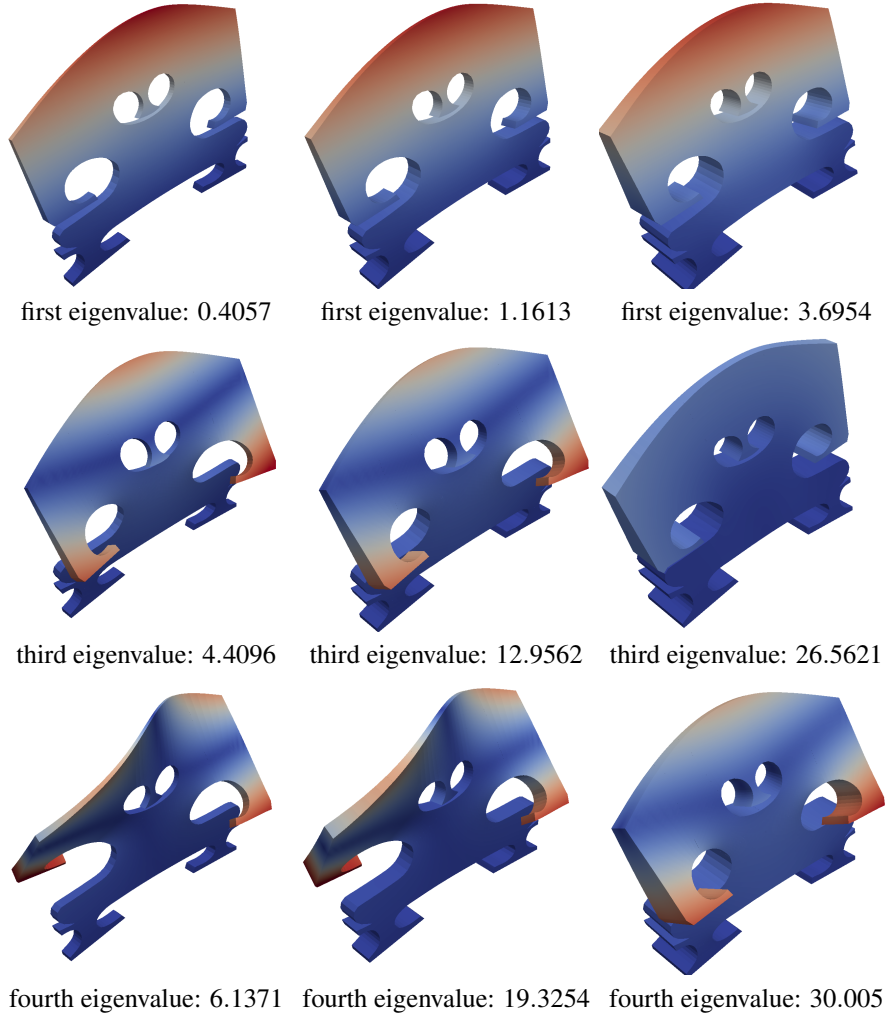


Figure 6: Influence of the thickness of the bridge on several eigenfunctions.

The first reduced basis test is the simultaneous approximation of the first five eigenpairs on both parameter-sets \mathcal{P}_1 and \mathcal{P}_2 . We use an initial basis of size 25 computed by a POD, which is enriched by the greedy algorithm up to a basis size of 250. In Figure 7, the error decay for the different eigenvalues and eigenfunctions is presented. We observe very good convergence, with a similar rate in all cases. As expected the magnitude of the error grows with the complexity of the parameter range.

Also an approximation of a larger number of eigenpairs does not pose any unexpected difficulties. Error values for the eigenvalue and eigenfunction are shown in Fig-

ure 8 for an approximation of the first 15 eigenpairs in the parameter-set \mathcal{P}_1 , showing a good convergence behavior. The reduced basis size necessary for a given accuracy increases compared to the previous cases of 5 eigenpairs, due to the higher amount of eigenfunctions which are, for a fixed parameter, orthogonal to each other.

When considering the relative error for the eigenvalues, see Figure 7 and Figure 8, we note that for a fixed basis size, the higher eigenvalues have a better relative approximation than the lower ones. In contrast, considering the eigenfunctions, the error of the ones associated with the lower eigenvalues are smaller compared to the ones associated with the higher eigenvalues. In Figure 9, we see the same effect, when considering absolute error values for the eigenvalue compared to the relative values. The error in the eigenfunctions has the same ordering as the absolute error in the eigenvalue. For the parameters under consideration, the lower and higher ones of the considered eigenvalues differ by magnitudes as illustrated in Figure 10. Hence when computing the relative error from the absolute ones, the error values of the high eigenvalues are divided by a large number and become small compared to the lower eigenvalues.

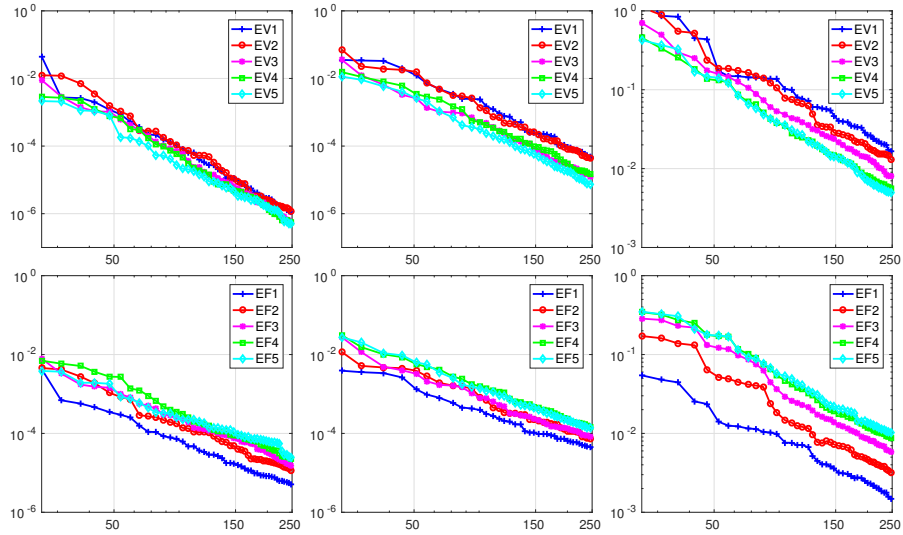


Figure 7: Convergence of the relative error of the eigenvalues (top) and eigenfunctions (bottom). Parameter range \mathcal{P}_1 with a fixed thickness (left), with varying thickness (middle) and parameter range \mathcal{P}_2 with varying thickness (right).

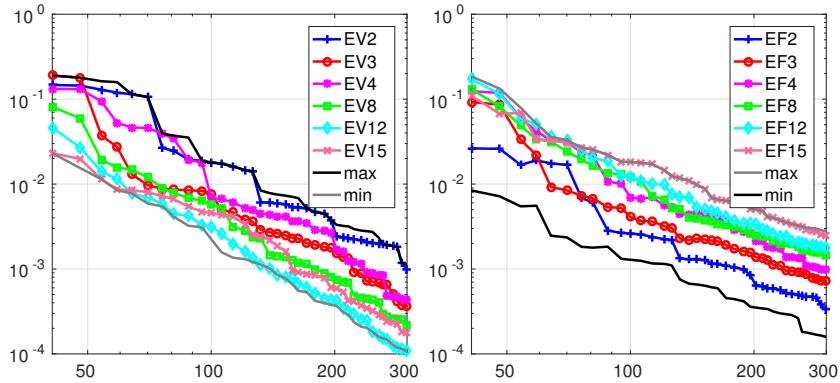


Figure 8: Convergence of the relative error of the eigenvalues (left) and eigenfunctions (right). Parameter range \mathcal{P}_1 with varying thickness, simultaneous approximating 15 eigenpairs.

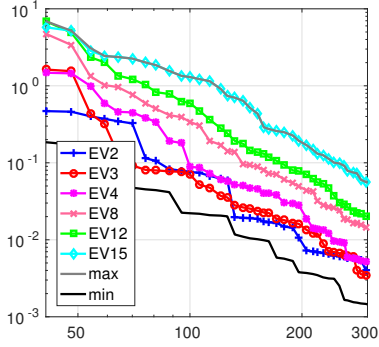


Figure 9: Convergence of the absolute error value for the eigenvalues. Parameter range \mathcal{P}_1 with varying thickness, simultaneous approximating 15 eigenpairs.

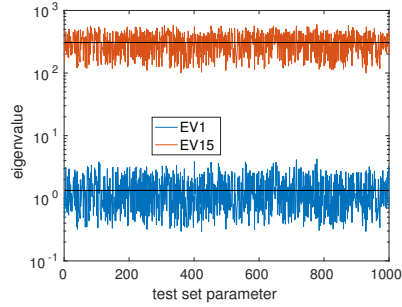


Figure 10: Sampling of the first and 15th eigenvalue within the parameter set \mathcal{P}_1 as used in the test set. Extremal values: $\min \lambda_1 = 0.29$, $\max \lambda_1 = 4.24$, $\min \lambda_{15} = 100.19$, $\max \lambda_{15} = 593.65$.

5 Conclusion

We have shown an eigenvalue reduced basis approximation of a violin bridge as an interesting application in vibroacoustic. The model reduction yields a good approximation quality in all cases of consideration, with a significant complexity reduction. The detailed system, a saddle point problem of 47,985 degrees of freedom, was reduced to a positive-definite system of less than 300 degrees of freedom. Furthermore, the thickness of the violin bridge, included as a geometry parameter, was shown to have a significant influence on the eigenvalues and eigenfunctions, without posing further difficulties to the reduced basis approximation. Altogether, it was shown that reduced basis methods are suitable for vibroacoustical mortar settings even with a parameter-dependent geometry.

References

- [1] L. BEIRÃO DA VEIGA, A. BUFFA, G. SANGALLI, AND R. VÁSQUEZ, *Mathematical analysis of variational isogeometric methods*, Acta Numerica, 23 (2014), pp. 157–287.
- [2] F. BEN BELGACEM, *The mortar finite element method with Lagrange multipliers*, Numer. Math., 84 (1999), pp. 173–197.
- [3] F. BEN BELGACEM AND Y. MADAY, *The mortar finite element method for three dimensional finite elements*, Math. Model. Numer. Anal., 31 (1997), pp. 289–302.
- [4] C. BERNARDI, Y. MADAY, AND A. T. PATERA, *A new nonconforming approach to domain decomposition: the mortar element method*, in Nonlinear partial differential equations and their applications., H. B. et.al., ed., vol. XI, Collège de France, 1994, pp. 13–51.
- [5] E. BRIVADIS, A. BUFFA, B. WOHLMUTH, AND L. WUNDERLICH, *Isogeometric mortar methods*, Comput. Methods Appl. Mech. Eng., 284 (2015), pp. 292–319.
- [6] J. A. COTTRELL, T. J. R. HUGHES, AND Y. BAZILEVS, *Isogeometric Analysis. Towards Integration of CAD and FEA*, Wiley, Chichester, 2009.
- [7] C. DE FALCO, A. REALI, AND R. VÁSQUEZ, *GeoPDEs: A research tool for isogeometric analysis of PDEs*, Adv. Eng. Softw., 42(12) (2011), pp. 1020–1034.
- [8] M. DITTMANN, M. FRANKE, I. TEMIZER, AND C. HESCH, *Isogeometric analysis and thermomechanical mortar contact problems*, Comput. Methods Appl. Mech. Eng., 274 (2014), pp. 192–212.
- [9] W. DORNISCH, G. VITUCCI, AND S. KLINKEL, *The weak substitution method an application of the mortar method for patch coupling in nurbs-based isogeometric analysis*, International Journal for Numerical Methods in Engineering, 103 (2015), pp. 205–234.
- [10] M. DROHMANN, B. HAASDONK, S. KAULMANN, AND M. OHLBERGER, *A software framework for reduced basis methods using DUNE -RB and RBmatlab*, Advances in DUNE, (2012), pp. 77–88.
- [11] N. H. FLETCHER AND T. ROSSING, *The physics of musical instruments*, Springer-Verlag, New York, 2nd ed., 1998.
- [12] I. FUMAGALLI, A. MANZONI, N. PAROLINI, AND M. VERANI, *Reduced basis approximation and a posteriori error estimates for parametrized elliptic eigenvalue problems*, ESAIM: M2AN, (2016).
- [13] A.-L. GERNER AND K. VEROY, *Certified reduced basis methods for parametrized saddle point problems*, SIAM Journal on Scientific Computing, 34 (2012), pp. A2812–A2836.
- [14] S. GLAS AND K. URBAN, *On non-coercive variational inequalities*, SIAM J. Numer. Anal., 52 (2014), p. 22502271.

- [15] S. GLAS AND K. URBAN, *Numerical investigations of an error bound for reduced basis approximations of noncoercive variational inequalities*, IFAC-PapersOnLine, 48 (2015), pp. 721 – 726.
- [16] B. HAASDONK, J. SALOMON, AND B. WOHLMUTH, *A reduced basis method for parametrized variational inequalities*, SIAM Journal of Mathematical Analysis, 50 (2012), pp. 2656–2676.
- [17] C. HESCH AND P. BETSCH, *Isogeometric analysis and domain decomposition methods*, Comput. Methods Appl. Mech. Eng., 213–216 (2012), pp. 104–112.
- [18] T. HORGER, B. WOHLMUTH, AND T. DICKOPF, *Simultaneous reduced basis approximation of parameterized elliptic eigenvalue problems*, ESAIM: Mathematical Modelling and Numerical Analysis, (2016). published online.
- [19] T. J. R. HUGHES, J. A. COTTRELL, AND Y. BAZILEVS, *Isogeometric analysis: CAD, finite elements, NURBS, exact geometry and mesh refinement*, Comput. Methods. Appl. Mech. Eng., 194 (2005), pp. 4135–4195.
- [20] T. J. R. HUGHES, J. A. EVANS, AND A. REALI, *Finite element and NURBS approximations of eigenvalue, boundary-value, and initial-value problems*, Comput. Methods Appl. Mech. Eng., 272 (2014), pp. 290–320.
- [21] L. IAPICHINO, A. QUARTERONI, G. ROZZA, AND S. VOLKWEIN, *Reduced basis method for the Stokes equations in decomposable domains using greedy optimization*, ECMI 2014, (2014), pp. 1 – 7.
- [22] A. LOVGREN, Y. MADAY, AND E. RONQUIST, *A reduced basis element method for the steady Stokes problem*, M2AN Math. Model. Numer. Anal., 40 (2006), pp. 529–552.
- [23] L. MACHIELS, Y. MADAY, I. B. OLIVEIRA, A. T. PATERA, AND D. V. ROVAS, *Output bounds for reduced-basis approximations of symmetric positive definite eigenvalue problems*, C. R. Acad. Sci., Paris, Sér. I, 331 (2000), pp. 153–158.
- [24] R. MILANI, A. QUARTERONI, AND G. ROZZA, *Reduced basis method for linear elasticity problems with many parameters*, Comput. Methods Appl. Mech. Eng., 197 (2008), pp. 4812 – 4829.
- [25] F. NEGRI, A. MANZONI, AND G. ROZZA, *Reduced basis approximation of parametrized optimal flow control problems for the Stokes equations*, Computers & Mathematics with Applications, 69 (2015), pp. 319 – 336.
- [26] G. PAU, *Reduced-basis method for band structure calculations*, Phys. Rev. E, 76 (2007), p. 046704.
- [27] G. PAU, *Reduced Basis Method for Quantum Models of Crystalline Solids*, PhD thesis, Massachusetts Institute of Technology, June 2007.
- [28] G. PAU, *Reduced basis method for simulation of nanodevices*, Phys. Rev. B, 78 (2008), p. 155425.
- [29] A. QUARTERONI, *Numerical Models for Differential Problems*, vol. 8 of MS&A, Springer, Milan, 2nd ed., 2014.

- [30] A. QUARTERONI, A. MANZONI, AND F. NEGRI, *Reduced Basis Methods for Partial Differential Equations. An Introduction*, Springer, 2015.
- [31] O. RAND AND V. ROVENSKI, *Analytical Methods in Anisotropic Elasticity: with Symbolic Computational Tools*, Birkhäuser, 2007.
- [32] T. RANZ, *Ein feuchte- und temperaturabhängiger anisotroper Werkstoff: Holz*, Beiträge zur Materialtheorie, Universität der Bundeswehr München, 2007.
- [33] G. ROZZA, D. B. P. HUYNH, AND A. MANZONI, *Reduced basis approximation and a posteriori error estimation for Stokes flows in parametrized geometries: roles of the inf-sup stability constants*, Numerische Mathematik, 125 (2013), pp. 115–152.
- [34] G. ROZZA, D. B. P. HUYNH, AND A. T. PATERA, *Reduced basis approximation and a posteriori error estimation for affinely parametrized elliptic coercive partial differential equations. Application to transport and continuum mechanics.*, Arch. Comput. Methods Eng., 15 (2008), pp. 229–275.
- [35] G. ROZZA AND K. VEROY, *On the stability of the reduced basis method for Stokes equations in parametrized domains*, Comput. Methods. Appl. Mech. Eng., 196 (2007), pp. 1244–1260.
- [36] A. SEITZ, P. FARAH, J. KREMHELLER, B. WOHLMUTH, W. WALL, AND A. POPP, *Isogeometric dual mortar methods for computational contact mechanics*, Comput. Methods Appl. Mech. Eng., 301 (2016), pp. 259–280.
- [37] S. VALLAGHE, D. P. HUYNH, D. J. KNEZEVIC, T. L. NGUYEN, AND A. T. PATERA, *Component-based reduced basis for parametrized symmetric eigenproblems*, Adv. Model. Simul. Eng. Sci., 2 (2015).
- [38] J. WOODHOUSE, *On the "bridge hill" of the violin*, Acta Acustica united with Acustica, 91 (2005), pp. 155–165.